Published in final edited form as:
Neurobiol Dis. 2012 March ; 45(3): 1031–1041. doi:10.1016/j.nbd.2011.12.022.

The abolishment of anesthesia-induced cognitive impairment by timely protection of mitochondria in the developing rat brain: the importance of free oxygen radicals and mitochondrial integrity

A Boscolo[1,2], **JA Starr**[1], **Sanchez V**[1,3], **N Lunardi**[1,2], **MR DiGruccio**[1,3], **C Ori**[2], **A Erisir**[3,4], **P Trimmer**[5,6], **J Bennett**[5,7], and **Jevtovic-Todorovic V**[1,3]

[1]Dept. of Anesthesiology, University of Virginia, Charlottesville, VA

[2]Dept. of Anesthesiology and Pharmacology, University of Padova, Padova, Italy

[3]Neuroscience Graduate Program, University of Virginia, Charlottesville, VA

[4]Dept. of Psychology, University of Virginia, Charlottesville, VA

[5]Parkinson's Disease Center, Virginia Commonwealth University, Richmond, VA

[6]Dept. of Anatomy and Neurobiology, Virginia Commonwealth University, Richmond, VA

[7]Dept. of Neurology, Virginia Commonwealth University, Richmond, VA

Abstract

Early exposure to general anesthesia (GA) causes developmental neuroapoptosis in the mammalian brain and long-term cognitive impairment. Recent evidence suggests that GA also causes functional and morphological impairment of the immature neuronal mitochondria. Injured mitochondria could be a significant source of reactive oxygen species (ROS), which, if not scavenged in timely fashion, may cause excessive lipid peroxidation and damage of cellular membranes. We examined whether early exposure to GA results in ROS upregulation and whether mitochondrial protection and ROS scavenging prevent GA-induced pathomorphological and behavioral impairments. We exposed 7-day-old rats to GA with or without either EUK-134, a synthetic ROS scavenger, or R(+) pramipexole (PPX), a synthetic aminobenzothiazol derivative that restores mitochondrial integrity. We found that GA causes extensive ROS upregulation and lipid peroxidation, as well as mitochondrial injury and neuronal loss in the subiculum. As compared to rats given only GA, those also given PPX or EUK-134 had significantly downregulated lipid peroxidation, preserved mitochondrial integrity, and significantly less neuronal loss. The subiculum is highly intertwined with the hippocampal CA1 region, anterior thalamic nuclei, and both entorhinal and cingulate cortices; hence, it is important in cognitive development. We found that PPX or EUK-134 co-treatment completely prevented GA-induced cognitive impairment. Because mitochondria are vulnerable to GA-induced developmental

Corresponding Author: Vesna Jevtovic-Todorovic, Department of Anesthesiology, University of Virginia Health System, PO Box 800710, Charlottesville, VA 22908, USA, Phone 434-924-2283; Fax 434-982-0019, vj3w@virginia.edu.

Commercial Interest: Dr. Bennett is the inventor on multiple patents protecting the use of R(+) PPX and receives royalty payments from those patents. Patents protecting use of R(+)PPX have been licensed to Knopp Biosciences and Biogen-Idec. Neither company provided support for this study or was involved in data collection, data analysis or manuscript preparation. Drs. Bennett and Jevtovic-Todorovic have applied for patent protection regarding use of R(+)PPX to prevent GA-induced cell death.

neurotoxicity, they could be an important therapeutic target for adjuvant therapy aimed at improving the safety of commonly used GAs.

Keywords

isoflurane; lipid peroxidation; reactive oxygen species; EUK-134; pramipexole; learning/memory

Introduction

Early exposure to general anesthesia (GA) causes widespread apoptotic neurodegeneration in the developing mammalian brain (Jevtovic-Todorovic et al., 2003; Rizzi et al., 2008; Slikker et al., 2007). Animal and human data also suggest an association between early exposure to GA and long-term impairment of cognitive development (Jevtovic-Todorovic et al., 2003; Fredriksson et al. 2004; 2007; Kalkman et al., 2009; Wilder et al., 2009).

The triggering events in GA-induced developmental neuroapoptosis are being extensively investigated. Activation of the intrinsic mitochondria-dependent apoptotic pathway appears to be the earliest sign of neuronal injury (Yon et al., 2005). Our recently published evidence that GA causes significant morphological impairment of mitochondria in the developing rat brain supports the finding that mitochondria are subcellular targets of GA (Lunardi at al., 2010)

Mitochondria, especially dysfunctional ones, are a formidable source of reactive oxygen species (ROS), which, if not scavenged quickly enough, can cause serious oxidative damage; that damage is manifested as excessive lipid peroxidation. Interestingly, mitochondrial DNA, unlike nuclear DNA, has a limited oxidative damage repair mechanism. This makes mitochondria especially vulnerable to damage caused by increased ROS production (Reddy and Beal, 2005).

Mitochondrial dysfunction and excessive ROS production are important in the development and progression of several degenerative diseases, including Alzheimer's disease, Parkinson's disease and Huntington's disease, known to be plagued by severe cognitive decline (Bennett, 2005; Reddy 2007; Trushina et al., 2004). Consequently, natural antioxidants and ROS scavengers have been shown to slow the advance of cognitive deterioration (reviewed by Calabrese et al., 2010). Because of their high oxygen requirements and relative deficiency in oxidative defenses (particularly low to moderate activity of catalase and Mn-superoxide dismutase-SOD), neurons are highly sensitive to excessive ROS production.

In view of the evidence that GA causes functional and morphological impairment of the immature mitochondria, we asked: 1) Does GA-induced mitochondria damage result in upregulation of ROS? 2) Does GA-induced ROS upregulation result in membrane lipid peroxidation? 3) Does protection of mitochondrial integrity and ROS scavenging guard against GA-induced mitochondria injury? 4) Is protection of mitochondrial integrity important in preventing neuronal loss? 5) Does effective mitochondrial protection result in the restoration of neuronal function (i.e., behavioral cognitive function)?

To address these questions, we exposed 7-day-old rats to GA. During the peri-anesthesia period, we also exposed rats to either EUK-134, a synthetic ROS scavenger having both Mn-SOD and catalase activity (Liu et al., 2003; Baker et al., 1998), or R(+) pramipexole [R(+) PPX], a synthetic aminobenzothiazol derivative that blocks permeability transition

pores, restores the integrity of mitochondrial membranes (Sayeed et al., 2006), and limits ROS production (Cassarino et al., 1998; Zuo et al., 2000; Le et al., 2000).

Materials and Methods

Animals

Sprague-Dawley rat pups at postnatal day (PND) 7 were used for anesthesia administration, since this is when they are most vulnerable to anesthesia-induced neuronal damage (Yon et al., 2005). We exposed PND 7 rats of both sexes to one of six treatment protocols, each 6 h in duration: 1) sham controls (21% oxygen + vehicle, 0.1% DMSO); 2) GA-treated (midazolam, 9 mg/kg, i.p.; single injection given immediately before the administration of 0.75% isoflurane + 75% nitrous oxide + about 24% oxygen); 3) GA + EUK-134-treated [EUK-134 at 10 mg/kg, s.c.; total of two doses were administered – first, 24 h and second dose 30 min prior to GA]; 4) EUK-134 alone (same dosing regimen); 5) GA + PPX-treated (PPX at 1 mg/kg, i.p.; total of four doses - the first dose was given 9 h before GA; the second dose immediately before GA; the third dose immediately after GA and the fourth dose 9 h after GA); and 6) PPX alone (same dosing regimen). At the end of the assigned treatment, rat pups were reunited with their mothers. Each day, we noted their general appearance and body weight.

Post-anesthesia rats were randomly divided into three groups: 1) for behavioral studies such as the radial arm maze-RAM and open field test (OFT); 2) for histomorphological studies, including ultrastructural analyses, detection of ROS, and neuronal density analysis; and 3) for biochemical studies of lipid peroxidation, such as 8-isoprostane synthesis. All experiments were approved by the Animal Care and Use Committee of the University of Virginia Health System and were done in accordance with the Public Health Service's Policy on Human Care and Use of Laboratory Animals. All efforts were made to minimize the number of animals used.

Anesthesia and drugs

N_2O and oxygen (GTS Welco, Richmond, VA) were delivered using gas-specific calibrated flowmeters. Isoflurane was administered using an agent-specific vaporizer that delivers a set percentage of anesthetic. Midazolam (Sigma-Aldrich Chemical, St. Louis, MO) was dissolved in 0.1% dimethyl sulfoxide (DMSO) just before administration. For control animals, 0.1 % DMSO was used. To administer a specific concentration of nitrous oxide (N_2O)/oxygen and isoflurane in a highly controlled environment, we used an anesthesia chamber (Yon et al., 2005; Lu et al., 2006). Rats were kept normothermic throughout the experiment (Jevtovic-Todorovic et al., 2000). For control experiments, air (GTS Welco, Richmond, VA) was substituted for the gas mixture. After initial equilibration of the N_2O/oxygen/isoflurane (experimental condition) or air (sham control condition) atmosphere inside the chamber, the composition of the chamber gas was analyzed using an infrared analyzer (Datex Instruments, Baldwin Park, CA) to establish the concentrations of N_2O, isoflurane, carbon dioxide, and oxygen.

EUK-134 (Carman Chemical, Ann Arbor, Michigan) was dissolved in DMSO (0.1%). R(+)PPX was custom manufactured by Quality Chemical Laboratories (Wilmington, NC) and was dissolved in normal saline.

Histopathological studies

Ultrastructural Electron Microscopy studies—In this study, we focused on the subiculum because, as part of the hippocampus proper and Papez's circuit, it is intertwined with the hippocampal CA1 region, anterior thalamic nuclei, and both entorhinal and

cingulate cortices. Accordingly, the subiculum is important in cognitive development, especially the development of learning and memory (McNaughton, 2006). Beyond that the subiculum is exquisitely vulnerable to GA-induced developmental neuroapoptosis (Jevtovic-Todorovic et al., 2003; Rizzi et al., 2008), resulting in a significant loss of neurons (Nikizad et al., 2007; Rizzi et al., 2008) and synapses (Lunardi et al., 2010) in later stages of synaptogenesis.

On PND 21, each pup was deeply anesthetized with Nembutal (65 mg/kg, i.p.). After cannulating the left ventricle, we clamped the descending aorta and did an initial flush with Tyrodes solution (30–40 ml), followed by 10 min of continuous perfusion with freshly prepared paraformaldehyde (4%) and glutaraldehyde (0.5%), following standard procedures (Jevtovic-Todorovic et al., 2003; Yon et al., 2005; 2006; Lu et al., 2006). The brains were removed and stored in the same fixative overnight. Both control and experimental pups were perfused on the same day, using the same solution to minimize variability in perfusates. Fixed brains were coronally sectioned (50–75 μm thick) with a DTK-1000 microslicer (Ted Pella, Tools for Science and Industry, Redding CA). Sections containing subiculum in each brain were localized based on standard anatomical atlases (Paxinos and Watson, 1944), and they were fixed in 2% osmium tetroxide (EM Sciences, Hatfield, PA), stained with 4% uranyl acetate (EM Sciences), and embedded in between two aclar sheets using epon-araldite resin (Electron Microscopy Sciences, Hatfield, PA). The subiculi were then dissected from the aclar sheets and reembedded in beam capsules. To prepare ultrathin sections, capsules embedded sections were trimmed and re-sectioned (silver interference color, 600–900 Å) on a Sorvall MT-2 microtome (Ivan Sorvall, Norwalk, CT), using a diamond knife (Diatome, Hatfield, PA). These sections were placed on copper grids and examined using a JEOL 1010 transmission electron microscope. Using a 16M-pixel digital camera (SIA-12C digital cameras, Scientific Instruments and Applications, Duluth, GA), we took random, nonoverlapping electron micrographs (12,000 × magnification) of subicular neuropil (total of 10–12 electron micrographs per animal; n=3 rats per group). The investigator taking and analyzing electron micrographs was blinded to the experimental conditions. To quantify the ultrastructural effects of the assigned treatment on mitochondria we assessed their morphological appearance and assigned them as being normal or 'abnormal' using the following four criteria: 1) continuation of mitochondrial outer and inner membrane: if intact – it was scored as normal; if broken – it was scored as damaged or 'abnormal'; 2) roundness of the mitochondrial envelope: the ones with round envelope were counted as normal; the ones with spiky corners were counted as abnormal; 3) discernability of cristae: if more than one cristae with both membranes intact was discernable than the mitochondrion was counted as normal; if one or no cristae had both membranes intact or their matrix appeared vacuolated mitochondrion was counted as abnormal; 4) the signs of degeneration: electron dense and dark profiles without clear outline between the inner and outer membrane were counted as abnormal. To be counted as abnormal each mitochondrion had to fulfill at least one of the criteria indicative of damage. The percentage of abnormal mitochondria in subicular neuropil was derived from the ratio between the number of abnormal mitochondria and total mitochondria in subicular neuropil. The data are presented as mean + SEM.

Evaluation of intracellular ROS formation—The formation of reactive oxygen species (mainly superoxide and hydrogen ions) was detected using an oxidant-sensing fluorescent probe, 2′,7′-dichlorofluorescin diacetate (H2DCF -DA, Sigma-Aldrich, St. Louis, MO) immediately post-anesthesia. This probe is de-esterified within cells by endogenous esterases to the ionized free acid 2′,7′-dichlorofluorescin; 2′,7′-dichlorofluorescin (DCF), which is then oxidized to fluorescent DCF by hydroperoxides (Hempel et al. 1999). DCF was easily detected and quantified using a green filter at a wavelength of 458 nm. Immediately post-anesthesia PND 7 rats were sacrificed and their brains sliced using a

DTK-1000 microslicer (Ted Pella, Tools for Science and Industry, Redding GA). Fresh sagittal slices (200 μm) were immediately placed in 10mM H_2DCF-DA (molecular probe C6827) and incubated for 45 min at 37°C, then rinsed in PBS (Liu et al., 2003). The laser fluorescent DCF-images were analyzed using a confocal scope (Zeiss LSM 510, Carl Zeiss MicroImaging GmbH, Germany) after being captured on photo multiplier tubes and transferred to the computer screen. Fluorescence was measured in each confocal image by focusing on the pyramidal subicular layer while using soma size as an important parameter (soma diameter larger than 12 – 15 um). The number of fluorescence-labeled pyramidal neurons was determined using imagePro Plus 5.1 software and expressed per mm^2.

Light microscopy—To determine the neuronal density in the subicular pyramidal layer, each group of rats was euthanized on PND 53, when the subiculum is fully developed. After being deeply anesthetized, rats were immediately perfused with 4% paraformaldehyde in 0.1M phosphate buffer at pH 7.4. The brains were fixed overnight, stored in 70% ethanol, blocked in paraffin, cut in 8-μm sections and Nissl-stained.

Quantitative histology—To determine the density of neurons, a counting frame (0.036 × 0.036 mm) and a high numerical aperture objective lens were used to visualize neurons. Once a subicular pyramidal neurons were identified, three random areas within that region were subsampled using Image-Pro Plus 5.1 computer software, which enabled us to count all neuronal profiles with equal probability of their being included in the sample only once. Unbiased subsampling was done by randomly selecting 10–12 viewing fields in each area (Rizzi et al., 2008). The counting frame was positioned at different focal levels in three different coronal sections. The numerical density of Nissl-stained neurons in each group of rats was expressed as the number of cells/mm^2 (Nikizad et al., 2007; Rizzi et al., 2008). The counting was done by an investigator who was blind to the experimental conditions.

Statistical analyses—Neuronal density, mitochondrial density and ROS labeling were assessed using ANOVA models that included, as a between-subject variable, the treatment groups. When ANOVAs with repeated measures were needed, the Bonferroni correction was used to help maintain prescribed alpha levels (e.g. 0.05).

Quantification of pg 8-isoprostane

Each group of rats was sacrificed immediately postanesthesia and the brains quickly removed. The subcortical region was dissected, snap-frozen in liquid nitrogen, and stored at −80°C. Levels of pg 8-isoprostane in the brain tissue were assayed using a commercially available enzyme immunoassay (EIA) kit (Cayman Chemical, Ann Arbor, MI). The frozen brains were allowed to thaw for 15 min in 1 mL ice-cold 0.1M phosphate buffer, pH 7.4, containing 1mM EDTA and 0.05% BHT. Each sample was homogenized for 15 sec using a polytron-type homogenizer. Each sample (250 uL) was transferred to a new centrifuge tube and hydrolyzed by the addition of 250 ul of 15% KOH. The samples were incubated at 40°C for 60 min. We added 1.5 ml of 1M phosphate buffer, pH 7.2, to each sample. The pH of samples was tested to ensure a pH within a range of 7.0–7.4. The samples were centrifuged at 8,000 rpm for 10 min at 4°C. The supernatant, diluted by a factor of 2 with EIA buffer, was used immediately for the assay.

The assay was done following the manufacturer's instructions and using the 96-well ELISA plate provided. Absorbance was read at 405 nm. Data were analyzed using a software package provided by the manufacturer and a four- parameter logistic curve fit. Total protein was measured for each sample on the day of the assay using a commercially available protein determination kit (Bradford method) (Cayman Chemical, Ann Arbor, MI).

Behavioral studies

Radial Arm Maze—To assess the cognitive effects of our treatments, we utilized the radial arm maze (RAM) test. This test, commonly used to evaluate spatial and reference memory in rodents, can detect subtle changes in learning and memory caused by anesthetics and sedatives (Palanisamy et al., 2011; Ward et al. 1999). Each arm of the 8 arm-RAM was baited with a food reward (chocolate cereal). The rats were food-restricted (with free access to water) from PND 45 to PND 73 (when RAM testing was completed), to achieve 85%–90% of their ad libitum weight (see Fig. 6, also Jevtovic-Todorovic et al., 2003). Visual cues were provided to assist spatial navigation. Rats were given 21 days to reach criterion; that is, to give 8 correct responses (retrieve a food reward placed in each arm) out of the first 9 responses for 4 consecutive days of testing. If a rat did not reach the criterion during the allotted time, it was assigned a score of 25 days (Rothstein et al. 2008).

Open Field Test—To assess locomotor activity, we subjected rats to the open field test (OFT) on PND 32. The OFT apparatus (36 × 36 inches) consists of 25 equal-size squares. Rats were allowed to acclimatize to the environment for at least 1 h before starting the activity counts. Each rat was placed in a corner of the field; its number of zone entries and rears on hind legs were recorded for 5 min. Total activity counts are the sum of the zone entries (horizontal exploration) and rears (vertical exploration) (Lau et al. 2008).

Statistical Analysis—Data from each behavioral test were subjected to an ANOVA involving treatment and gender as between-subject variables and blocks of trials as within-subject variables. Pairwise comparisons were done after the significant effects of treatment and other relevant variables, as well as *p* values exceeding Bonferroni corrected levels, were noted. Using the standard version of GraphPad 5.01 software, we considered $p < 0.05$ to be statistically significant.

Results

The time points for behavioral testing and tissue collections are indicated in the following descriptions of the protocols used. Since we found no difference between sexes at the ages chosen for testing, the data are compiled from both sexes.

I. Early exposure to GA caused upregulation of ROS in the subiculi that was significantly diminished by the ROS scavenger, EUK-134

These studies were based on a report that the impairment of mitochondrial integrity is one of the first signs of neuronal dysfunction after anesthesia exposure (Yon et al., 2005). Since dysfunctional mitochondria could be a strong source of free oxygen radicals, we examined whether GA induces a significant upregulation of ROS. We sacrificed PND 7 rats from the Sham, GA and GA+EUK-134 groups immediately after the assigned treatment (within 2–3 minutes) and obtained freshly cut subicular sagittal slices (200 μm thick). These slices were stained with H_2-DCFDA dye, which detects ROS- hydrogen peroxide and SOD ions in particular. As shown in Fig. 1A, the pyramidal layer (the boundaries are roughly outlined) in the sham control subiculum displays only a few H_2-DCFDA-positive pyramidal neurons, whereas H_2-DCFDA-positive profiles (green fluorescence) are abundant in the pyramidal layer of GA-treated animals (Fig. 1B). Quantification demonstrated an approximately 10- to 11-fold increase in the number of ROS-positive pyramidal neurons compared to those in sham controls (Fig. 1D; $p < 0.001$). As predicted, EUK-134 treatment curtailed GA-induced upregulation of ROS as shown by significant decrease in ROS labeling in the pyramidal layer (Fig. 1C) of GA + EUK-treated rats. This decrease was approximately 5-fold as compared to the number in GA-treated animals ($p < 0.01$) (Fig. 1D). As a result, ROS labeling was not significantly higher in GA+EUK-treated rats as compared to shams (p =

0.10). We conclude that GA significantly upregulates ROS in the developing subiculum, while EUK-134 scavenges GA-induced ROS upregulation.

II. GA-induced upregulation of ROS in subiculi resulted in profound lipid peroxidation, which was significantly ameliorated by the ROS scavenger, EUK-134

To assess whether GA-induced ROS upregulation leads to peroxidation of lipid membranes in subicular tissue, we quantified the production of pg 8-isoprostane, the most abundant prostaglandin-like compound formed in vivo from free radical-catalyzed peroxidation of essential fatty acids (primarily arachidonic acid). The level of the pg 8-isoprostane in GA-treated animals was significantly increased as compared to that in sham controls ($p < 0.05$) and EUK-alone groups ($p < 0.01$) (Fig. 2). However, co-treatment with EUK-134 resulted in significant downregulation in lipid peroxidation manifested as a more than 2-fold decrease in pg 8-isoprostane content in the GA+EUK-group as compared to the GA-alone group ($p < 0.001$). This indicates that EUK-induced ROS downregulation protects cell membranes from GA-induced lipid peroxidation.

III. Early exposure to GA caused morphological damage to mitochondria, which was reversed by co-treatment with either EUK-134 or PPX

To determine whether substantial ROS upregulation accompanied by significant lipid peroxidation of cellular and subcellular membranes affects mitochondrial structural integrity, we examined the ultrastructure of mitochondria. We paid special attention to changes indicating mitochondrial inner-outer membrane damage in subiculular neurons from rats in our six treatment groups.

Qualitative examination of neuropil of GA-treated subiculi at 14 days after anesthesia (PND 21) revealed many mitochondria that were swollen with balloon-like cristae (Fig. 3A). Due to inner mitochondrial membrane disintegration, mitochondrial matrices appeared disorganized and vacuolated (early stage, open arrows) (left panel). Other mitochondrial profiles were electron dense and they displayed no clear outline between the inner and outer membranes (late stage shown by closed arrows in left and right panels). In contrast to GA-treated subiculi, mitochondrial profiles in GA + EUK- (Fig. 3B) and GA + PPX-treated (Fig. 3C) PND 21 rats appeared similar to controls with intact inner and outer membranes. The lack of characteristics of degenerating mitochondria suggested that treatment with EUK-134 or PPX around the time of GA exposure offered complete and lasting protection against GA-induced morphological changes.

To confirm this notion we performed the quantification analysis of abnormal-looking mitochondria in subicular neuropil of each treatment group. We found that the percentage of abnormal-looking mitochondria in GA-treated animals was 2-fold higher compared to sham controls ($p< 0.001$, Fig. 3D). When the protective effects of either EUK-134 or PPX treatments were quantified we confirmed that there was significantly lower density of abnormal-looking mitochondria in either group when compared to GA-treated group ($p< 0.001$) (Fig. 3D). The protection was of such degree that the percentage of abnormal-looking mitochondria approached the percentage detected in sham control group thus making GA +EUK or GA+PPX group practically indistinguishable from sham controls. When we quantified the densities of abnormal-looking mitochondria in EUK-134 or PPX alone group we found no difference compared to sham controls (data not shown) (n=3 rats in each treatment group).

When the morphological appearance of neuropil was assessed we found that both EUK-134 and PPX treatment protected developing subicular neuropil as well. The strikingly disorganized appearance of neuropil in GA-treated animals (Fig. 4B), which had many

swollen neuron-glia profiles, appeared to be completely protected in the GA + EUK-treated (Fig. 4C) and GA + PPX-treated groups (Fig. 4D). Note the abundance of degenerated mitochondria in GA-treated neuropil (Fig. 4B, closed arrows) as well as the presence of disorganized microtubules bunched in the periphery of neuron-glia profiles (asterisks). Due to extensive swelling, the microtubules often had vacuolar appearance (open arrows). None of these pathomorphological features were detected in GA + EUK-treated (Fig. 4C) and GA + PPX-treated groups (Fig. 4D). Indeed, it was impossible to distinguish neuropil in these two groups from sham control neuropil (Fig. 4A). Similarly, neuropil in the EUK-134- and PPX-alone groups were indistinguishable from those in sham controls (data not shown) (n=3 rats per group).

IV. Neuronal deletion in subiculi caused by early exposure to GA was prevented with EUK-134 or PPX treatment

Because GA induces not only severe ROS upregulation and lipid peroxidation, but also substantial ultrastructural damage to mitochondria and neuropil, we examined whether these changes have long-term consequences with regard to neuronal survival manifested as potential neuronal loss. In rats by PND 53, synaptogenesis is complete and cellular debris from GA-induced damage has already been removed (Nikizad et al., 2007). Consequently, we examined remaining neuronal density in the pyramidal layer of subiculi in PND 53 rats, looking for presumably permanent changes. Using Nissl staining, we quantified neuronal density in the pyramidal layers of rat subiculum from all six treatment groups. We found significant neuronal loss in GA-treated rats as compared to sham controls ($p < 0.01$) (Fig. 5). Overall neuronal loss in GA-treated rats varied from 40% to 50%. Treatment with either EUK-134 or PPX around the time of GA exposure prevented neuronal loss; i.e., the GA +EUK-134 and GA+PPX groups had levels of neuronal density that were similar to levels in sham controls and significantly higher than levels in rats treated with GA alone ($p < 0.01$). Neuronal densities in the EUK-134-alone and PPX-alone groups were indistinguishable from those in sham controls (data not shown).

To determine whether acute GA-induced ROS upregulation and lipid peroxidation, in addition to long-term impairment of mitochondrial integrity and neuronal loss are important in GA-induced cognitive impairment, selected behavioral assessments were performed in each experimental group once rats reached adolescence and young adulthood.

V Early exposure to GA did not impair rat nutritional development

Since proper nutritional status is critically important for cognitive development, we compared the overall appearance and daily weight of rats in each group. Based on their general appearance, rats in different groups could not be distinguished from each other. Similarly, there was no difference in daily weight gain between the groups (Fig. 6). The time points when the animals were treated (PND 7), food restricted (from PND 45), tested on the radial arm maze (RAM) (from PND 53) and permitted to eat ad libitum (from PND 73) are indicated on the graph. Food restriction, a necessary component of the RAM learning protocol, was limited so that no rat lost more than 10%–15% of its body weight.

VI. Early exposure to GA induced long-term cognitive impairment that was completely prevented by EUK-134, a ROS scavenger, and PPX, a mitochondria protector

To assess the effect of GA-induced ROS upregulation on cognitive development, we tested the spatial working memory of rats in the six treatment groups using the 8-arm RAM test. GA-treated rats were significantly impaired relative to sham controls ($p < 0.001$) in terms of days required to reach a criterion demonstrating learning (8 correct responses out of the first 9 responses for 4 consecutive days) (Fig. 7A). As compared to rats in the GA-treated group, those in the GA + EUK-treated group showed a significant decrease in the number of days

required to reach criterion ($p < 0.001$) (Fig. 7B), indicating not only improvement in learning, but complete prevention against GA-induced learning impairment; i.e., the GA +EUK group was indistinguishable from sham controls (Fig. 7A). Similarly, rats given PPX at the time of GA treatment showed significant improvement in learning as compared to rats in the GA-treated group ($p < 0.001$) (Fig. 7C), resulting in RAM learning ability being indistinguishable from that among sham controls (Fig. 7A). As shown in Figs. 7B and C, the learning ability of rats in the EUK-134- and PPX-alone groups, respectively was similar to that of sham controls (Fig. 7A). For the clarity of pairwise statistical comparisons, same GA–treated group was plotted in all three parts of Figure 7.

Graphing RAM data in terms of the cumulative percentage of rats reaching criterion as a function of blocks of trials (2 days per block) (Fig. 8A) showed that the acquisition rate of the GA-treated group (closed squares) began to slow down as compared to that of sham controls (closed triangles) by the fourth block of trials and remained substantially slower for the remainder of training. In contrast, rats in the GA + EUK- (closed circle) and GA + PPX-treated (closed inverted triangles) groups initially exhibited slightly faster acquisition than did those in the sham control group although, after the 5^{th} block of trials, their learning curves closely trailed the learning curve of sham controls. While 15% of GA rats (5 out of 35) did not learn the task during the allotted 21 days, all sham control rats did so several days before the cut-off point. Whereas all 20 rats in the GA + PPX- group completed the task, 2 of the 26 rats (about 7%) in the GA + EUK-134 group did not. We conclude that co-treatment of GA rats with either EUK or PPX resulted in normalization of the acquisition rate. The EUK- and PPX-only groups were practically indistinguishable from sham controls (data not shown).

To further assess how the RAM learning curve of GA-treated rats compares to other treatment groups, we plotted the cumulative percent scores for GA-treated animals relative to recorded cumulative percent scores for other treatment groups, using a percent-percent plot (p-p plot) (Fig. 8B). We found that when only 51% of GA-treated rats had reached criterion, 90% sham controls had mastered the task. Furthermore, when only 79% of GA-treated rats had reached criterion, all sham controls and GA+PPX animals as well as 93% of GA+EUK animals had mastered the task. We conclude that both EUK-134 and PPX co-treatment closed the gap (shaded area) in learning ability between GA-treated (lower dotted line) and sham-control animals (upper dotted line).

VII. Early exposure to GA did not cause hyperactivity

To examine whether GA treatment causes changes in horizontal and vertical explorations, a commonly used measure of hyperactivity and anxiety, we tested the six groups of rats at PND 32 using an open field test. Total activity (the number of horizontal and vertical explorations in 5 min) was unchanged in all treatment groups compared to sham controls (data not shown). Similarly, when horizontal and vertical explorations were plotted individually, there was no difference between the groups (data not shown).

Discussion

GA administered during brain development caused significant upregulation of ROS, which was accompanied by considerable membrane lipid peroxidation, mitochondria damage, and neuronal loss in the subiculi of young rats. ROS scavenging with EUK-134 or protection of mitochondria with R(+) PPX around the time of anesthesia exposure resulted in significant downregulation of ROS and lipid peroxidation, as well as prevention of mitochondrial morphological damage, protection of neuropil, and prevention of neuronal loss. Most importantly, peri-anesthesia treatment with EUK-134 or R(+) PPX prevented anesthesia-induced cognitive impairment.

Morphologically distorted and functionally impaired mitochondria generate excessive ROS and reduce ATP production, thereby damaging neurons (Reddy, 2006). Our earlier in-vivo findings indicated that GA increases mitochondria membrane permeability in part by downregulating bcl-x_L protein levels, thus causing cytochrome-c leakage and caspase-cascade activation (Yon et al., 2005). Increasing evidence suggests that ROS have a key role in promoting cytochrome-c release from mitochondria (Nishimura et al., 2001; Petrosillo et al., 2011; 2003; Galindo et al., 2003), indicating that GA-induced cytochrome-c leakage can also be caused by excessive GA-induced ROS upregulation. Although the temporal relationship between ROS upregulation and cytochrome c leak remains to be established it appears that a crucial (and perhaps the initial) cellular target of GA-induced developmental neurodegeneration is immature mitochondria, which seem to be damaged by multiple means converging to induce long-lasting detrimental effects on developing neurons.

Mitochondrial dysfunction and excessive ROS production, accompanied by significant peroxidation of cellular and subcellular lipid membranes, are important in the development and progression of several neuronal diseases marked, among other symptoms and signs, by severe cognitive decline (Reddy, 2006; 2007; Trushina et al., 2004; Bennett, 2005). Neurons are highly dependent on glucose for ATP synthesis and produce ROS as byproducts of oxidative phosphorylation within mitochondria. At the same time, neurons, because of their high oxygen requirements and relative deficiency in oxidative defenses (in particular, low to moderate activity of catalase and Mn-SOD), are highly sensitive to excessive ROS production. This vulnerability, combined with their high content of polyunsaturated fatty acids, makes them susceptible to excessive lipid peroxidation and cellular damage (Halliwell, 1992). Here we have presented evidence that early exposure to GA makes developing neurons susceptible to ROS-induced mitochondria-propagated lipid peroxidation that may be consequential for the observed neuronal injury and impairment of proper cognitive development. Based on significant prevention of GA-induced pathomorphological and cognitive impairments by EUK-134 and R(+) PPX, therapeutic interventions aimed at decreasing ROS production, preventing excessive lipid peroxidation and protecting mitochondria could be the key to safe use of GA during early stages of brain development. This is of particular interest considering the fact that the exposure to GA is often a planned event where a safening agent could be co-administered in timely fashion. Such neuroprotective strategies should enable the use of general anesthetics to their full therapeutic potential while potentially avoiding long-term neuronal damage and/or cognitive sequellae.

The possibility that GA is a direct ROS producer cannot be excluded. For example, N_2O, which is one of the anesthetics used in our regimen can generate free oxygen (most likely hydroxy) radicals in the presence of trace metals such as iron and copper (Orestes et al., 2011), both commonly found in biological fluids and neurons. Upregulation of ROS promotes metal-catalyzed protein oxidation, which in turn permanently alters the function of various cellular proteins (Stadtman and Berlett, 1991; Stadtman, 1993). For example, N_2O causes inhibition of low-voltage-activated calcium channels by oxidizing critical amino acids in the functional pore of the channel (Orestes et al., 2011). However, having considered that possibility we believe that it is unlikely that N_2O production of ROS and potential protein oxidation is the main culprit for developmental neurotoxicity we present in this study. For example, our previous work using N_2O as a sole anesthetic in clinically relevant concentrations (up to 180-vol%) has shown no detrimental effects on neuronal integrity nor any signs of neuronal apoptosis during early stages of brain development (Jevtovic-Todorovic et al., 2003). Nevertheless, some degree of N_2O-induced ROS generation, combined with mitochondria-induced ROS production resulting from GA-induced mitochondrial impairment may overwhelm the scavenging system, initiating the cascade of events in which mitochondria becomes not only a target, but also a culprit.

Two agents that we have chosen to study, EUK-134 and R(+) PPX, have distinct properties. EUK-134, a synthetic ROS scavenger with both Mn-SOD and catalase activity, catalytically eliminates both superoxide and hydrogen peroxide (Gonzales et al., 1995), but does not directly protect mitochondria. It is a potent and stable agent with a high degree of bioavailability which has been shown to offer neuroprotection against excessive ROS production in several in-vivo (Baker et al., 1998; Rong et al., 1999; Tiwari et al., 2009) and in-vitro (Fonck et al., 2003; Pong et al., 2002) models of neuronal injury. Here, for the first time, we show that EUK-134 decreases GA-induced ROS upregulation and, most importantly, blocks GA-induced learning impairment during development.

Whereas EUK-134 mainly scavenges ROS in the cytoplasm, thus indirectly protecting mitochondria and other organelles, R(+) PPX is a direct protector of mitochondrial integrity that scavenges superoxide anions inside the organelle. It easily crosses the blood-brain barrier, concentrates in the brain at about a 6-fold higher concentration than it does in plasma, and is taken up by mitochondria, where it is concentrated more than 8-fold (Danzeisen et al, 2006). Of particular interest here is that R(+) PPX, as opposed to S(−) PPX, has minimal dopaminergic activity. Accordingly, it has no apparent toxicity or significant side effects at very high doses. For example, the LD_{50} for i.p. R(+) PPX in rodents is ~375 mg/kg (unpublished observation), which is more than 80-fold higher than the combined four doses used in our protocol to abolish GA-induced cognitive impairment. Importantly, R(+) PPX has been used in clinical trials and has been shown to slow the progression of clinically documented amyotrophic lateral sclerosis without causing harmful side effects (Wang et al., 2008).

Since proper function of developing neurons relies on a fine balance between ROS production and elimination, the wellbeing of mitochondria and proper function of the scavenging system are crucially important. Consequently, protective interventions based on tight control of ROS production and/or elimination could be the earliest defenses against the progression of mitochondria damage to further ROS production, ATP depletion, caspase activation, and DNA fragmentation. Although the net effects of EUK-134 and R(+) PPX are ROS downregulation and curtailing of lipid peroxidation, those effects could be considered direct in the case of the EUK-134 and perhaps indirect in the case of R(+) PPX. In using these two agents, our goal was to examine the temporal role of ROS scavenging versus the protection of mitochondria integrity. We hypothesized that if EUK-134, a Mn-SOD/catalase mimetic, proved to be more effective in alleviating GA-induced developmental neurotoxicity, then GA's initial attack could be aimed at the complex scavenging system. By promoting effective and timely ROS elimination, EUK-134 treatment blocks ROS upregulation and ROS-induced mitochondria damage thus preventing further ROS upregulation. On the other hand, if R(+) PPX was shown to be more effective, the initial damage could be due to mitochondria dysfunction. Since both treatments were very effective when administered at the time of GA exposure, it may well be that GA-induced developmental neurotoxicity is a complex combination of extensive ROS production and impaired ROS scavenging that are tightly intertwined. Indeed, Guo et al. (2008) have proposed a "double jeopardy" in leptin-deficiency models of diabetes where the worsening of mitochondrial function leads to enhanced ROS production in tandem with impaired expression or function of scavenging machinery.

Although the focus of our study was on downstream consequences of mitochondrial impairment and upregulation in ROS it is noteworthy that the upstream trigger of a vicious cascade of mitochondrial damage could be the excessive release of calcium from the endoplasmic reticuli (EM) resulting in intacytosolic and mitochondrial calcium overload. This in turn may cause cytochrome c leak (Hanson et al., 2004) which could further promote mitochondrial dysfunction. Indeed, Zhao and colleagues (2010) have shown that by

modulating inositol 1,4,5-trisphosphate receptors, isoflurane induces significant calcium release from the ER resulting in acute elevation of cytosolic calcium and modulation of mitochondrial bcl-x_L protein levels which in turn promoted apoptotic neuronal death in the immature rat brain. It remains to be established whether and how anesthesia-induced modulation of calcium homeostasis is affected by EUK-134 or R(+) PPX-co-administration.

Based on our findings, determination of a temporal relationship between GA exposure, ROS upregulation, and mitochondrial damage appears to have only theoretical importance, despite the logical notion that the best intervention should be one specific to preventing the very initial steps. If, for instance, mitochondria are the initial GA target, agents aimed at protecting mitochondria, such as R(+) PPX, would be the most selective therapeutic approach. If, however, ROS accumulation is the initial event, then ROS scavengers should be the first line of defense, so that ROS-induced mitochondria damage is never initiated. Nevertheless, it appears that peri-anesthesia exposure to a "safening agent," whether aimed at curtailing ROS production or promoting ROS elimination, offers equally impressive prevention against the multifaceted impairments caused by early exposure to GA. Thus, our work suggests that GA-induced developmental neurotoxicity is the result of a highly complex interaction between ROS-induced, mitochondria -propagated, and mitochondria-induced ROS-propagated cascades of events that ultimately lead to neuronal damage and behavioral impairment.

Protective strategies based on preserving mitochondrial integrity have been previously shown to provide significant downregulation of GA-induced developmental neurodegeneration. For example, both melatonin, a naturally occurring sleep hormone that upregulates bcl-xL (Yon et al., 2006), and carnitine, a nutritional supplement that protects mitochondria integrity (Zou et al., 2008) cause significant, although not complete, neuronal protection. However, neither agent is known to protect against GA-induced cognitive impairment.

We present evidence that GA-induced long-term cognitive impairments in immature rats are prevented by two agents, EUK-134 and R(+) PPX, both of which prevent excessive ROS upregulation. Deciphering the earliest and most vulnerable cellular targets and their relative importance in promoting long-term cognitive impairments is the key to effective intervention. This study points toward an attainable means of providing safe anesthesia to the youngest members of our society.

Conclusions

Early exposure to general anesthesia causes developmental neuroapoptosis in the mammalian brain and long-term cognitive impairment that is caused, at least in part, by mitochondrial damage and excessive free oxygen radical production. Consequently, timely mitochondrial protection and free oxygen scavenging prevents anesthesia-induced lipid peroxidation, preserves mitochondrial integrity, and prevents neuronal loss. Importantly, it completely prevents anesthesia-induced cognitive impairment.

Acknowledgments

This study was supported by the NIH/NICHD HD44517 (to V.J-T.), NIH/NICHD HD44517-S (to V.J-T.), Harold Carron endowment (to V.J-T), John E. Fogarty Award TW007423-128322 (to P.I. V.J-T.). V.J-T. was an Established Investigator of the American Heart Association. The authors thank Jan Redick and the Advanced Microscopy Facility at the University of Virginia Health System for technical assistance with electron microscopy and data analyses. The authors thank Alexander Peterkin and Nathan Naughton for technical assistance with open field study.

Abbreviations

GA	general anesthesia
ROS	reactive oxygen species
EUK-134	chloro[[2,2′-[1,2-ethanediylbis[(nitrilo-κN)methylidyne]]bis[6-methoxyphenolato-κO]]]-manganese
PPX	pramipexole
CA1	Cornu Ammonis area 1
DNA	deoxyribonucleic acid
Mn-SOD	manganese-superoxide dismutase
PND	post-natal day
DMSO	dimethyl sulfoxide
i.p	intra-peritoneal
s.c	subcutaneous
OFT	open field test
N_2O	nitrous oxide
H_2-DCF-DA	H_2-2′, 7′-dichlorofluorescin diacetate
PBS	phosphate buffered saline
pg 8-isoprostane	prostaglandin 8-isoprostane
EIA	enzyme immunoassay
EDTA	Ethylene-diamino-tetra-acetic acid
BHT	Butylated hydroxytoluene
KOH	Potassium Hydroxide
ELISA	Enzyme-linked Immunosorbent Assay
RAM	radial arm maze
p-p plot	probability-probability plot or percent-percent plot
ATP	Adenosine Tri-Phosphate
LD_{50}	median lethal dose

References

Baker K, Marcus CB, Huffman K, Kruk H, Malfroy B, Doctrow SR. Synthetic combined superoxide dismutase/catalase mimetics are protective as a delayed treatment in a rat stroke model: a key role for reactive oxygen species in ischemic brain injury. J Pharmacol Exp Ther. 1998; 284:215–21. [PubMed: 9435181]

Bennett MC. The role of alpha-synuclein in neurodegenerative diseases. Pharmacol Ther. 2005; 105:311–31. [PubMed: 15737408]

Calabrese V, Cornelius C, Mancuso C, Lentile R, Stella AM, Butterfield DA. Redox homeostasis and cellular stress response in aging and neurodegeneration. Methods Mol Biol. 2010; 610:285–308. [PubMed: 20013185]

Cassarino DS, Fall CP, Smith TS, Bennett JP Jr. Pramipexole reduces reactive oxygen species production in vivo and in vitro and inhibits the mitochondrial permeability transition produced by

the parkinsonian neurotoxin methylpyridinium ion. J Neurochem. 1998; 71:295–301. [PubMed: 9648878]

Danzeisen R, Schwalenstoecker B, Gillardon F, Buerger E, Krzykalla V, Klinder K, Schild L, Hengerer B, Ludolph AC, Dorner-Ciossek C, Kussmaul L. Targeted antioxidative and neuroprotective properties of the dopamine agonist pramipexole and its nondopaminergic enantiomer SND919CL2x [(+)2-amino-4,5,6,7-tetrahydro-6-Lpropylamino-benzathiazole dihydrochloride]. J Pharmacol Exp Ther. 2006; 316:189–99. [PubMed: 16188953]

Fonck C, Baudry M. Rapid reduction of ATP synthesis and lack of free radical formation by MPP+ in rat brain synaptosomes and mitochondria. Brain Res. 2003; 975:214–21. [PubMed: 12763610]

Fredriksson A, Archer T, Alm H, Gordh T, Eriksson P. Neurofunctional deficits and potentiated apoptosis by neonatal NMDA antagonist administration. Behav Brain Res. 2004; 153:367–376. [PubMed: 15265631]

Fredriksson A, Pontén E, Gordh T, Eriksson P. Neonatal exposure to a combination of N-methyl-D-aspartate and gamma-aminobutyric acid type A receptor anesthetic agents potentiates apoptotic neurodegeneration and persistent behavioral deficits. Anesthesiology. 2007; 107:427–36. [PubMed: 17721245]

Galindo MF, Jordán J, González-García C, Ceña V. Reactive oxygen species induce swelling and cytochrome c release but not transmembrane depolarization in isolated rat brain mitochondria. Br J Pharmacol. 2003; 139:797–804. [PubMed: 12813003]

Gonzalez PK, Zhuang J, Doctrow SR, Malfroy B, Benson PF, Menconi MJ, Fink MP. (1995) EUK-8, a synthetic superoxide dismutase and catalase mimetic, ameliorates acute lung injury in endotoxemic swine. J Pharmacol Exp Ther. 1995; 275:798–806. [PubMed: 7473169]

Guo Z, Jiang H, Xu X, Duan W, Mattson MP. Leptin-mediated cell survival signaling in hippocampal neurons mediated by JAK STAT3 and mitochondrial stabilization. J Biol Chem. 2008; 283:1754–63. [PubMed: 17993459]

Halliwell B. Reactive oxygen species and the central nervous system. J Neurochem. 1992; 59:1609–23. [PubMed: 1402908]

Hanson CJ, Bootman MD, Roderick HL. Cell signalling: IP3 receptors channel calcium into cell death. Curr Biol. 2004; 14:R933–5. [PubMed: 15530388]

Hempel SL, Buettner GR, O'Malley YQ, Wessels DA, Flaherty DM. Dihydrofluorescein diacetate is superior for detecting intracellular oxidants: comparison with 2′,7′-dichlorodihydrofluorescein diacetate, 5(and 6)-carboxy-2′,7′-dichlorodihydrofluorescein diacetate, and dihydrorhodamine 123. Free Radic Biol Med. 1999; 27:146–59. [PubMed: 10443931]

Jevtovic-Todorovic V, Benshoff N, Olney JW. Ketamine potentiates cerebrocortical damage induced by the common anaesthetic agent nitrous oxide in adult rats. Br J Pharmacol. 2000; 130:1692–1698. [PubMed: 10928976]

Jevtovic-Todorovic V, Hartman RE, Izumi Y, Benshoff ND, Dikranian K, Zorumski CF, Olney JW, Wozniak DF. Early exposure to common anesthetic agents causes widespread neurodegeneration in the developing rat brain and persistent learning deficits. J Neurosci. 2003; 23:876–882. [PubMed: 12574416]

Kalkman CJ, Peelen L, Moons KG, Veenhuizen M, Bruens M, Sinnema G, de Jong TP. Behavior and development in children and age at the time of first anesthetic exposure. Anesthesiology. 2009; 110:805–12. [PubMed: 19293699]

Lau AA, Crawley AC, Hopwood JJ, Hemsley KM. Open field locomotor activity and anxiety-related behaviors in mucopolysaccharidosis type IIIA mice. Behav Brain Res. 2008; 191:130–6. [PubMed: 18453006]

Le WD, Jankovic J, Xie W, Appel SH. Antioxidant property of pramipexole independent of dopamine receptor activation in neuroprotection. J Neural Transm. 2000; 107:1165–73. [PubMed: 11129106]

Liu R, Liu IY, Bi X, Thompson RF, Doctrow SR, Malfroy B, Baudry M. Reversal of age-related learning deficits and brain oxidative stress in mice with superoxide dismutase/catalase mimetics. Proc Natl Acad Sci U S A. 2003; 100:8526–31. [PubMed: 12815103]

Lu LXJH, Yon J-H, Carter LB, Jevtovic-Todorovic V. General anesthesia activates BDNF-dependent neuroapoptosis in the developing rat brain. Apoptosis. 2006; 11:1603–15. [PubMed: 16738805]

Lunardi N, Ori C, Erisir A, Jevtovic-Todorovic V. General anesthesia causes long-lasting disturbances in the ultrastructural properties of developing synapses in young rats. Neurotox Res. 2010; 17:179–88. [PubMed: 19626389]

McNaughton N. The role of the subiculum within the behavioural inhibition system. Behav Brain Res. 2006; 174:232–50. [PubMed: 16887202]

Nikizad H, Yon J-H, Carter LB, Jevtovic-Todorovic V. Early exposure to general anesthesia causes significant neuronal deletion in the developing rat brain. Annals of New York Academy of Sciences. 2007; 1122:69–82.

Nishimura G, Proske RJ, Doyama H, Higuchi M. Regulation of apoptosis by respiration: cytochrome c release by respiratory substrates. FEBS Lett. 2001; 505:399–404. [PubMed: 11576536]

Orestes P, Bojadzic D, Lee J, Leach E, Salajegheh R, Digruccio MR, Nelson MT, Todorovic SM. Free radical signalling underlies inhibition of CaV3. 2 T-type calcium channels by nitrous oxide in the pain pathway. J Physiol. 2011; 589:135–48. [PubMed: 21059758]

Paxinos, G.; Watson, C. The Rat Brain in Stereotaxic Coordinates. Academic Press; Australia: 1944.

Palanisamy A, Baxter MG, Keel PK, Xie Z, Crosby G, Culley DJ. Rats exposed to isoflurane in utero during early gestation are behaviorally abnormal as adults. Anesthesiology. 2011; 114:521–8. [PubMed: 21307768]

Petrosillo G, Ruggiero FM, Pistolese M, Paradies G. Reactive oxygen species generated from the mitochondrial electron transport chain induce cytochrome c dissociation from beef-heart submitochondrial particles via cardiolipin peroxidation. Possible role in the apoptosis. FEBS Lett. 2001; 509:435–438. [PubMed: 11749969]

Petrosillo G, Ruggiero FM, Di Venosa N, Paradies G. Decreased complex III activity in mitochondria isolated from rat heart subjected to ischemia and reperfusion: role of reactive oxygen species and cardiolipin. FASEB J. 2003; 17:714–716. [PubMed: 12586737]

Pong K, Rong Y, Doctrow SR, Baudry M. Attenuation of zinc-induced intracellular dysfunction and neurotoxicity by a synthetic superoxide dismutase/catalase mimetic, in cultured cortical neuron. Brain Res. 2002; 950:218–30. [PubMed: 12231247]

Rizzi S, Carter LB, Ori C, Jevtovic-Todorovic V. Clinical anesthesia causes permanent damage to the fetal guinea pig brain. Brain Pathology. 2008; 18:198–210. [PubMed: 18241241]

Reddy PH, Beal MF. Are mitochondria critical in the pathogenesis of Alzheimer's disease? Brain Res Rev. 2005; 49:618–32. [PubMed: 16269322]

Reddy PH. Mitochondrial oxidative damage in aging and Alzheimer's disease: implications for mitochondrially targeted antioxidant therapeutics. J Biomed Biotechnol. 2006; 2006:31372. [PubMed: 17047303]

Reddy PH. Mitochondrial dysfunction in aging and Alzheimer's disease: strategies to protect neurons. Antioxid Redox Signal. 2007; 9:1647–58. [PubMed: 17696767]

Rong Y, Doctrow SR, Tocco G, Baudry M. EUK-134, a synthetic superoxide dismutase and catalase mimetic, prevents oxidative stress and attenuates kainate-induced neuropathology. Proc Natl Acad Sci U S A. 1999; 96:9897–902. [PubMed: 10449791]

Rothstein S, Simkins T, Nuñez JL. Response to neonatal anesthesia: effect of sex on anatomical and behavioral outcome. Neuroscience. 2008; 152:959–69. [PubMed: 18329814]

Sayeed I, Parvez S, Winkler-Stuck K, Seitz G, Trieu I, Wallesch CW, Schönfeld P, Siemen D. Patch clamp reveals powerful blockade of the mitochondrial permeability transition pore by the D2-receptor agonist pramipexole. FASEB J. 2006; 20:556–8. [PubMed: 16407457]

Slikker W Jr, Zou X, Hotchkiss CE, Divine RL, Sadovova N, Twaddle NC, Doerge DR, Scallet AC, Patterson TA, Hanig JP, Paule MG, Wang C. Ketamine-induced neuronal cell death in the perinatal rhesus monkey. Toxicol Sci. 2007; 98:145–158. [PubMed: 17426105]

Stadtman ER, Berlett BS. Fenton chemistry. J Biol Chem. 1991; 266:17201–17211. [PubMed: 1894614]

Stadtman ER. Oxidation of free amino acids and amino acid residues in proteins by radiolysis and by metal-catalyzed reactions. Annu Rev Biochem. 1993; 62:797–821. [PubMed: 8352601]

Tiwari V, Kuhad A, Chopra K. Suppression of neuro-inflammatory signaling cascade by tocotrienol can prevent chronic alcohol-induced cognitive dysfunction in rats. Behav Brain Res. 2009; 203:296–303. [PubMed: 19464322]

Trushina E, Dyer RB, Badger JD 2nd, Ure D, Eide L, Tran DD, Vrieze BT, Legendre-Guillemin V, McPherson PS, Mandavilli BS, Van Houten B, Zeitlin S, McNiven M, Aebersold R, Hayden M, Parisi JE, Seeberg E, Dragatsis I, Doyle K, Bender A, Chacko C, McMurray CT. Mutant huntington impairs axonal trafficking in mammalian neurons in vivo and in vitro. Mol Cell Biol. 2004; 24:8195–209. [PubMed: 15340079]

Wang H, Larriviere KS, Keller KE, Ware KA, Burns TM, Conaway MA, Lacomis D, Pattee GL, Phillips LH 2nd, Solenski NJ, Zivkovic SA, Bennett JP Jr. R+ pramipexole as a mitochondrially focused neuroprotectant: initial early phase studies in ALS. Amyotroph Lateral Scler. 2008; 9:50–8. [PubMed: 18270879]

Ward MT, Stoelzel CR, Markus EJ. Hippocampal dysfunction during aging II: deficits on the radial-arm maze. Neurobiol Aging. 1999; 20:373–80. [PubMed: 10604430]

Wilder RT, Flick RP, Sprung J, Katusic SK, Barbaresi WJ, Mickelson C, Gleich SJ, Schroeder DR, Weaver AL, Warner DO. Early exposure to anesthesia and learning disabilities in a population-based birth cohort. Anesthesiology. 2009; 110:796–804. [PubMed: 19293700]

Yon J–H, Daniel-Johnson J, Carter LB, Jevtovic-Todorovic V. Anesthesia induces neuronal cell death in the developing rat brain *via* the intrinsic and extrinsic apoptotic pathways. Neuroscience. 2005; 35:815–827. [PubMed: 16154281]

Yon J-H, Carter LB, Reiter RJ, Jevtovic-Todorovic V. Melatonin reduces the severity of anesthesia-induced apoptotic neurodegeneration in the developing rat brain. Neurobiol Dis. 2006; 21:522–530. [PubMed: 16289675]

Zhao Y, Liang G, Chen Q, Joseph DJ, Meng Q, Eckenhoff RG, Eckenhoff MF, Wei H. Anesthetic-induced neurodegeneration mediated via inositol 1,4,5-trisphosphate receptors. J Pharmacol Exp Ther. 2010; 333:14–22. [PubMed: 20086058]

Zou L, Xu J, Jankovic J, He Y, Appel SH, Le W. Pramipexole inhibits lipid peroxidation and reduces injury in the substantia nigra induced by the dopaminergic neurotoxin 1-methyl-4-phenyl-1,2,3,6-tetrahydropyridine in C57BL/6 mice. Neurosci Lett. 2000; 281:167–70. [PubMed: 10704769]

Zou X, Sadovova N, Patterson TA, Divine RL, Hotchkiss CE, Ali SF, Hanig JP, Paule MG, Slikker W Jr, Wang C. The effects of L-carnitine on the combination of, inhalation anesthetic-induced developmental, neuronal apoptosis in the rat frontal cortex. Neuroscience. 2008; 151:1053–65. [PubMed: 18201836]

Highlights

1. Early exposure to general anesthesia impairs the immature neuronal mitochondria.
2. Anesthesia causes free oxygen radical upregulation and lipid peroxidation.
3. EUK-134 and R(+) pramipexole down regulate ROS and protect mitochondria.
4. EUK-134 and R(+) pramipexole prevent anesthesia-induced cognitive impairments.

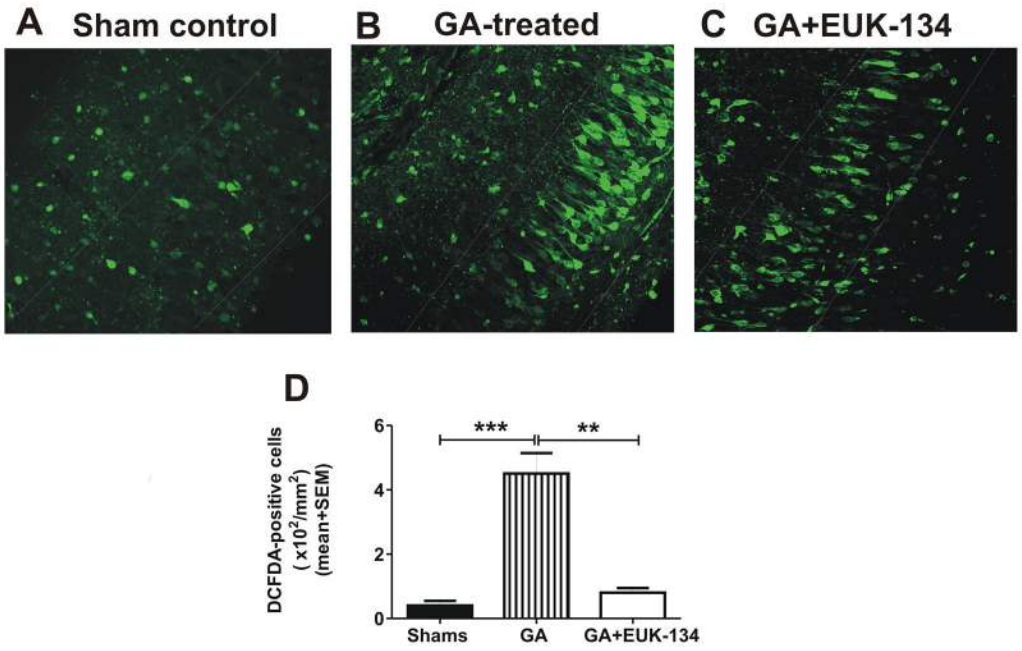

Figure 1. Anesthesia causes significant ROS upregulation in immature subiculi that is ameliorated by a synthetic scavenger, EUK-134

A. Subicular sagittal slices from sham control PND7 rats (A) displayed only a few H_2-DCFDA-positive pyramidal neurons (pyramidal layer is roughly outlined). **B.** There were abundant H_2-DCFDA-positive profiles (green fluorescence) in the pyramidal layer of GA-treated animals. **C.** EUK-134 co-treatment reduced GA-induced up-regulation of ROS. **D.** Quantification of ROS-positive pyramidal neurons showed significant upregulation in GA-treated subiculi compared to sham controls (***, $p < 0.001$). This was significantly diminished by EUK-134 co-treatment (~ 5-fold decrease compared to GA-treated animals; **, $p < 0.01$). Consequently, ROS labeling was not significantly higher in GA+EUK-treated animals than in shams (n = 4 rat pups per group).

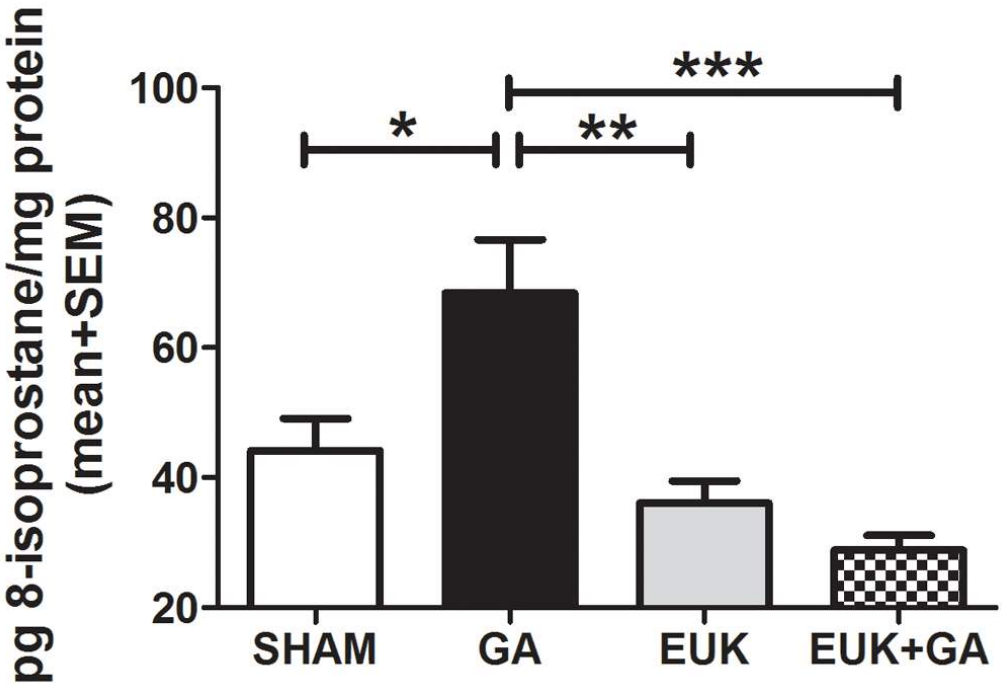

Figure 2. Significant anesthesia-induced lipid peroxidation in immature subiculi was reduced by EUK-134 co-treatment

Quantification of pg 8-isoprostane, the most abundant prostaglandin-like compound formed in vivo from the free-radical-catalyzed peroxidation of essential fatty acids (primarily arachidonic acid) showed significant upregulation in GA-treated rats compared to sham control (*, $p < 0.05$) and EUK-alone groups (**, $p < 0.01$). Co-treatment with EUK significantly downregulated pg 8-isoprostane production compared to that in the GA-alone group (over 2-fold) (***, $p < 0.001$) ($n = 5–6$ rat pups per group).

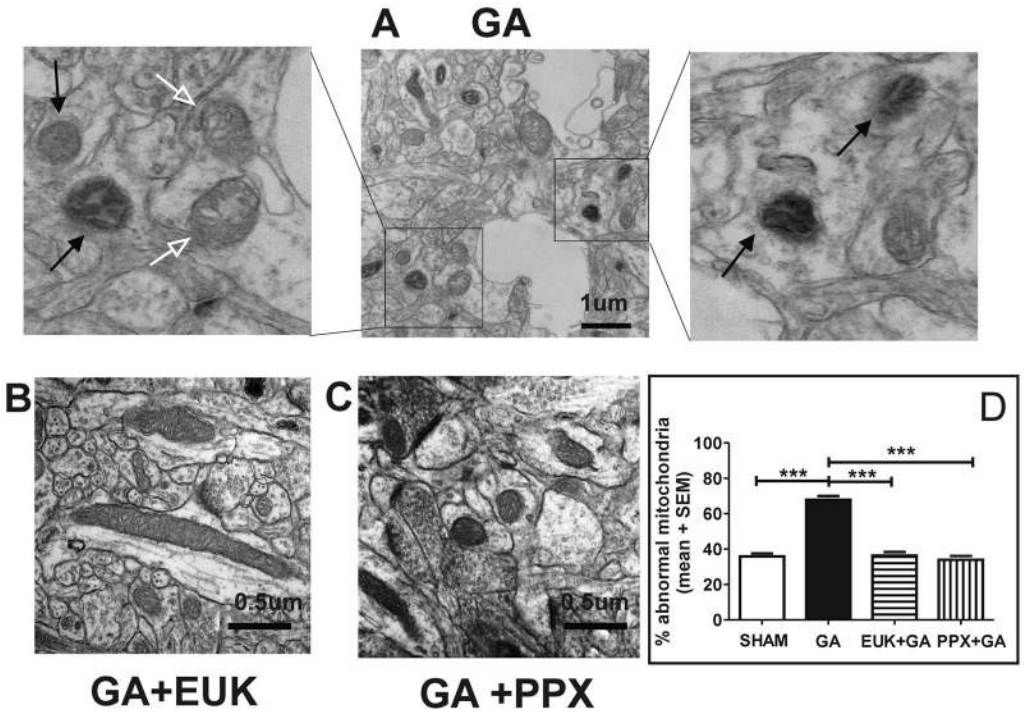

Figure 3. EUK-134 or R(+) PPX co-treatment prevented the significant morphological damage to subicular mitochondria caused by anesthesia

A. Neuropil of GA-treated subiculi analyzed 14 days after anesthesia (at PND 21) contained many swollen mitochondria with balloon-like cristae. **Left Enlargement:** The inner mitochondrial membrane appeared disintegrated, giving the mitochondrial matrix a disorganized and swollen look (early stage, open arrows). **Right enlargement:** Many mitochondrial profiles appear dark and condensed without a clear outline between the inner and outer membranes (late stage; closed arrows in left and right panels). **B.** Mitochondrial profiles in GA + EUK-treated and **C.** GA + PPX-treated subiculi show nicely stacked cristae with intact inner and outer membranes**. D. Mitochondrial density analyses revealed significant increase in the percentage of abnormal-looking mitochondria in GA-treated subicular neuropil compared to sham controls (p< 0.001). Co-treatment with either EUK-134 or PPX resulted in complete mitochondrial protection as indicated by a significant decrease in the density of abnormal-looking mitochondria (p< 0.001) when compared to GA-treated group. The protection was of such degree that GA+EUK and GA+PPX groups were practically indistinguishable from sham controls (n=3 rats per each treatment group).**

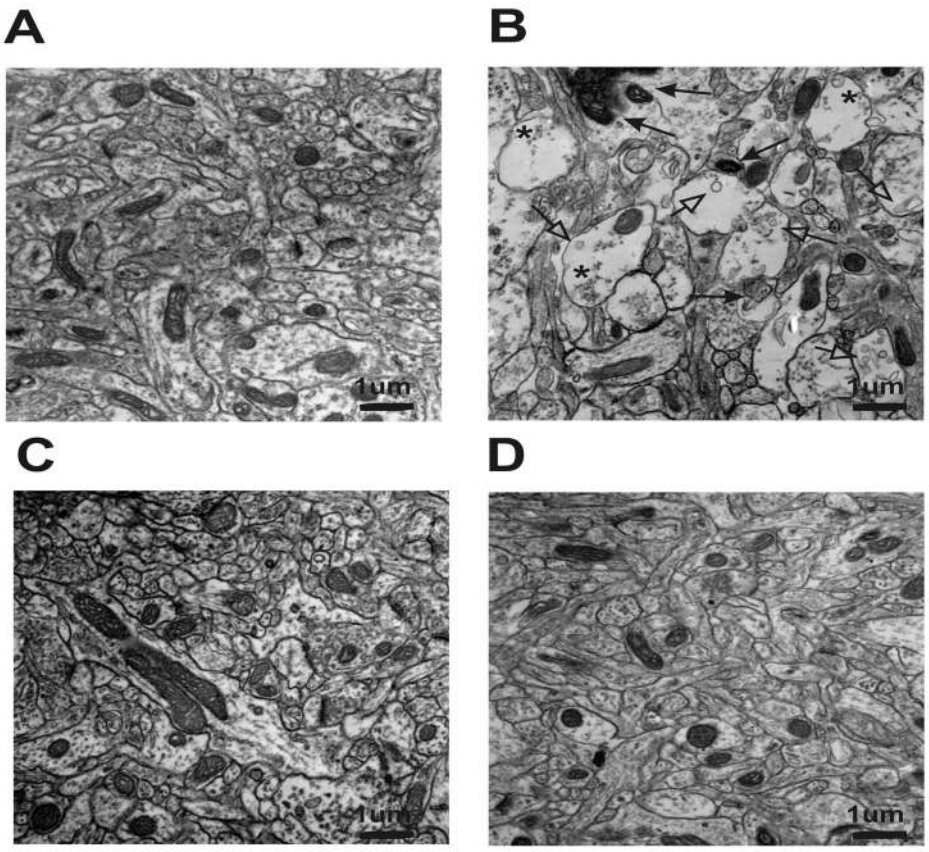

Figure 4. Significant anesthesia-induced disturbance of neuropil architecture in subiculi was prevented by EUK-134 or R(+) PPX co-treatment

A. Normal-looking sham control neuropil with tightly packed neuronal and glial profiles. **B.** The neuropil of GA-treated rat appears strikingly disorganized with numerous swollen neuron-glial profiles. There is an abundance of degenerated mitochondria in the neuropil (closed arrows). Many disorganized microtubules seem bunched in the periphery of neuron-glia profiles (asterisks). Due to extensive swelling, the microtubules often had vacuolar appearance (open arrows). **C.** Neuropil in GA + EUK- 134 treated and **D.** GA + PPX-treated groups were indistinguishable from sham control neuropil.

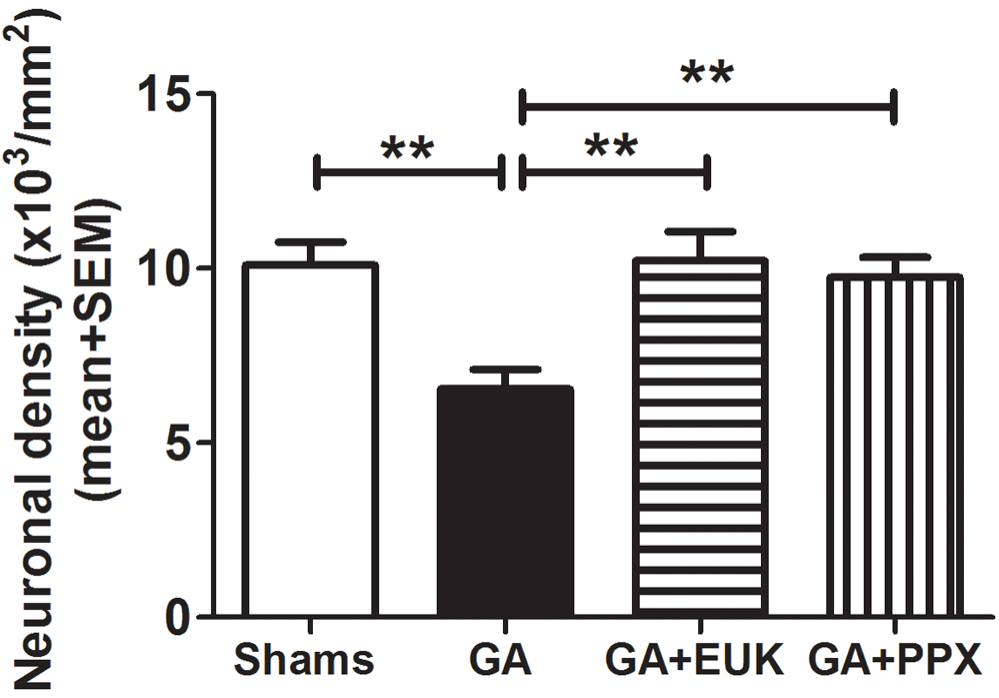

Figure 5. Significant anesthesia-induced neuronal deletion in subiculi was prevented by EUK-134 or R(+) PPX co-treatment

In PND 53 rats, there was significant (40%–50%) neuronal loss in GA-treated animals as compared to sham controls (**, $p < 0.01$). Treatment with either EUK-134 or PPX around the time of GA exposure prevented neuronal loss; i.e., the GA+EUK and GA+PPX groups had neuronal densities similar to those in sham controls and significantly higher than those in rats treated with GA alone (**, $p< 0.01$). (n = 4–6 animals per group).

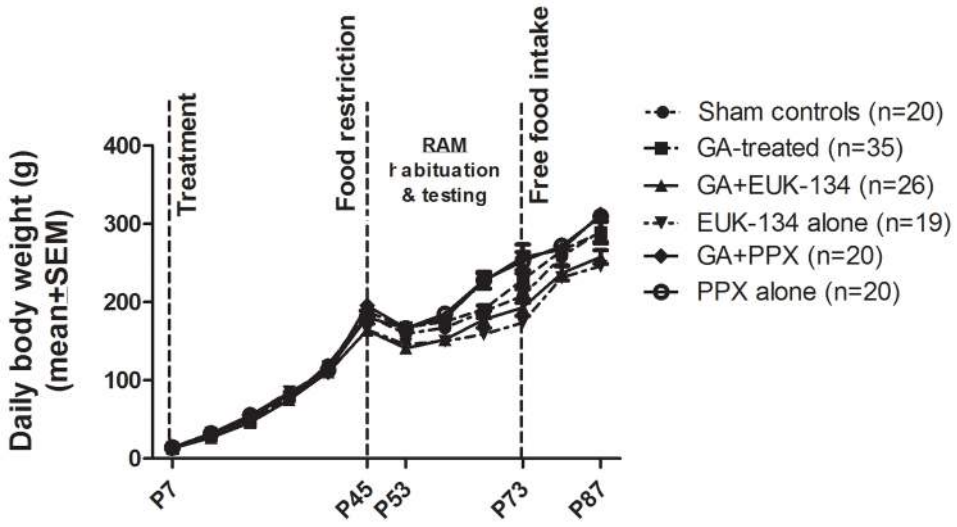

Figure 6. Anesthesia exposure did not impair rats' nutritional development

There were no differences in daily weight gain between treatment groups. Food restriction, a necessary component of the RAM learning protocol, caused no more than 10%–15% loss in body weight loss.

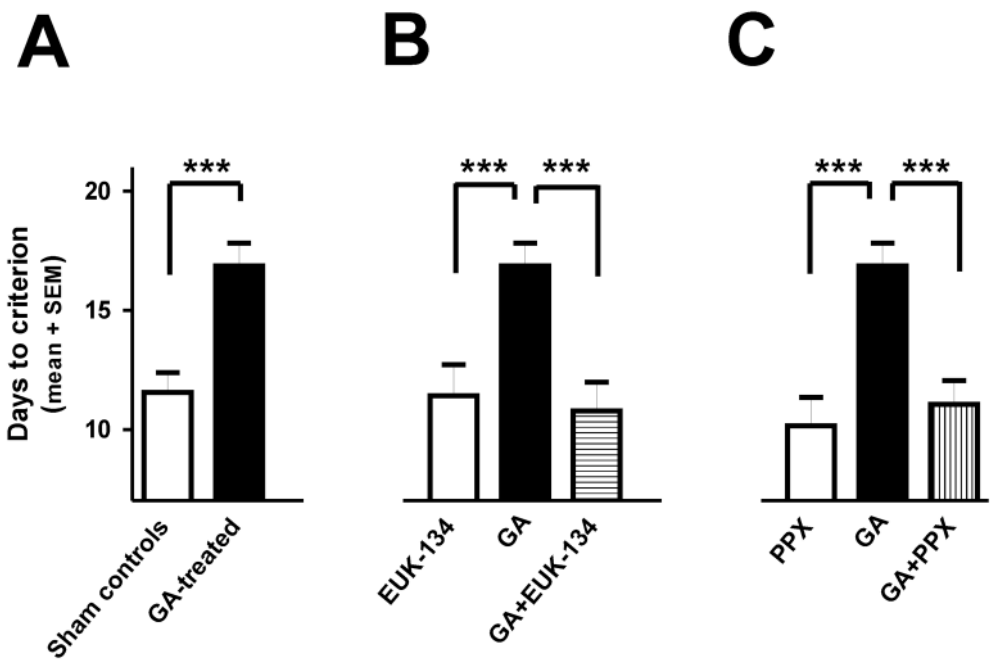

Figure 7. Significant cognitive impairment induced by early exposure to anesthesia was completely prevented by EUK-134 or R(+) PPX co-treatment

A. On the 8-arm RAM test, GA-treated rats were significantly impaired relative to sham controls (***, $p < 0.001$) in terms of days required to reach a criterion demonstrating learning (8 out of 9 correct responses for 4 consecutive days). **B.** The GA + EUK-treated group had a significant decrease in days required to reach criterion as compared to the GA-treated group (***, $p < 0.001$). There was no difference in learning when the GA+EUK group was compared to sham controls. **C.** The GA+PPX-treated group showed significant improvement in learning as compared to GA-treated group (***, $p < 0.001$). Comparison of the GA+PPX group to sham controls showed no difference in learning. The learning abilities of EUK-134- **(B)** and PPX-alone (C) groups were similar to sham controls (A) (n= 19–35 animals per group).

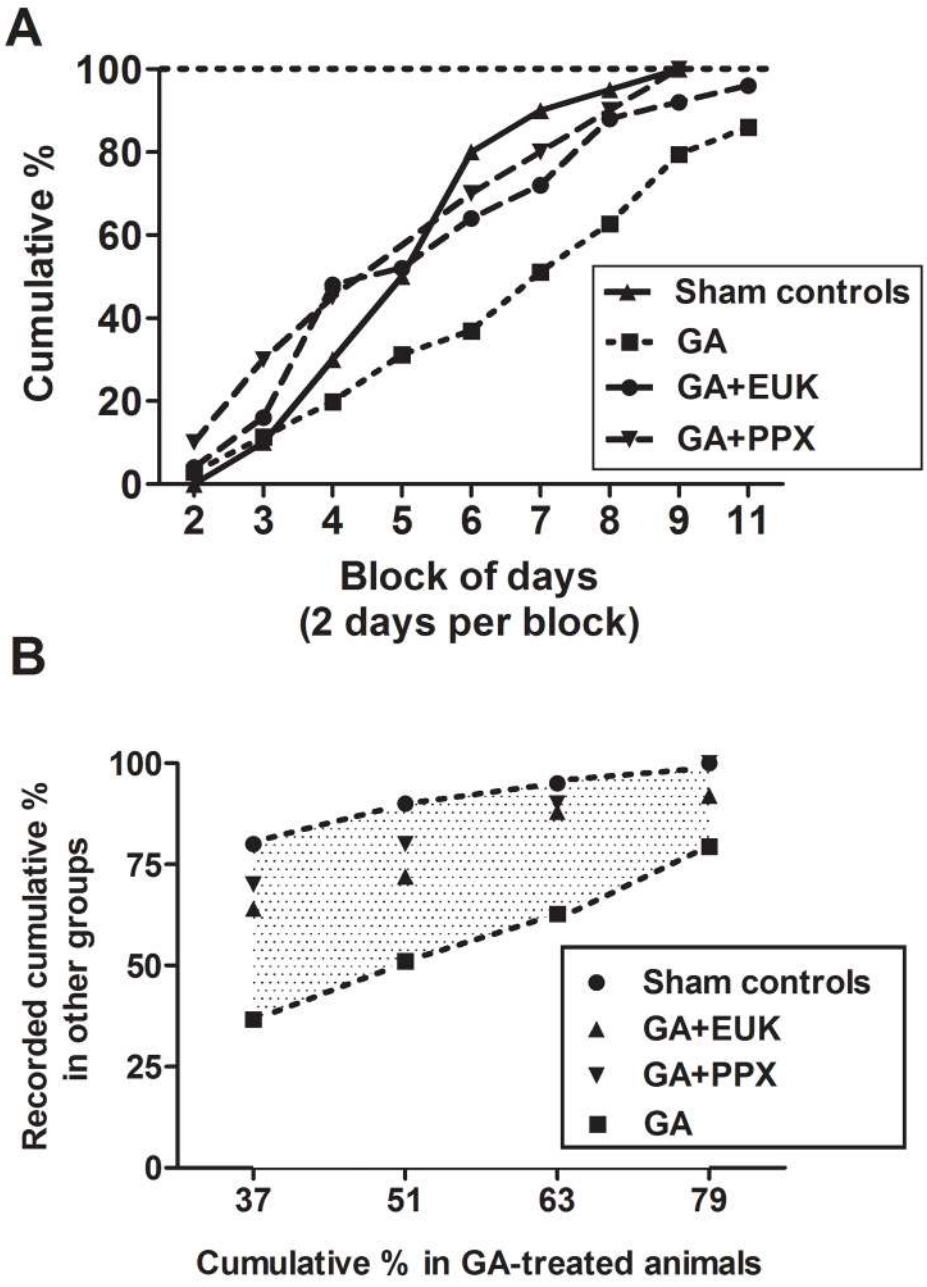

Figure 8. EUK-134 or R(+) PPX co-treatment prevented the slowing of learning acquisition induced by early anesthesia exposure

A. The acquisition rate of the GA-treated group (closed squares) began to slow as compared to that of sham controls (closed triangles) by the fourth block of trials and remained substantially slower for the remainder of training. GA + EUK- (closed circle) and GA + PPX-treated (closed inverted triangles) groups initially exhibited slightly faster acquisition than did the sham control group; after the 5th block of trials, their learning curve closely trailed that of sham controls. Five out of 35 (~ 15%) GA-treats rats did not learn the task during the 21 days allotted; all sham controls completed the task several days earlier. In the GA + PPX- group, all 20 animals completed the task. In the GA + EUK-134 group, 2 of 26 rats (~ 7%) did not learn the task. **B.** By plotting the cumulative scores for the GA-treated group relative to those for other treatment groups, we found that while only 51% of GA-

treated rats had reached the criterion, 90% of sham controls had done so. In addition, when only 79% of GA-treated rats had reached criterion, all sham controls and GA+PPX animals as well as 93% of GA+EUK animals had mastered the task. Either EUK-134 or PPX co-treatment closed the gap (shaded area) in learning abilities between GA-treated (lower dotted line) and sham-control animals (upper dotted line) (n = 19–35 animals per group).